DECOVALEX III TASK 2C: THERMAL-MECHANICAL MODELING OF THE DRIFT-SCALE HEATER TEST AT YUCCA MOUNTAIN—A PROGRESS REPORT

Prepared for

U.S. Nuclear Regulatory Commission
Contract NRC–02–97–009

Prepared by

Sui-Min Hsiung
Asadul H. Chowdhury

Center for Nuclear Waste Regulatory Analyses
San Antonio, Texas

December 2001

ABSTRACT

The drift-scale heater test at the Exploratory Studies Facility at Yucca Mountain is designated for study in Task 2 of the DECOVALEX III project. A NRC/CNWRA research team is involved in Subtasks 2A and 2C modeling activities. After completion of the thermal-hydrological analysis of the drift-scale heater test in Subtask 2A in May 2001, the preliminary activities of Subtask 2C began in the later part of fiscal year 2001. This progress report is in the form of a work plan for the Subtask 2C activities. The technical approach discussed herein was presented at the DECOVALEX III Annual Workshop in Naantali, Finland, October 22–26, 2001.

The work for Subtask 2C includes four major activities: (i) development of numerical models, (ii) compilation of material and strength properties data, (iii) production of numerical analyses, and (iv) preparation of reports.

The NRC/CNWRA research team will conduct thermal-mechanical modeling using both continuum and discontinuum approaches. The ABAQUS finite element computer program will be used for continuum analysis and the dda_ct2 discontinuous deformation analysis computer code for discontinuum analysis.

Development of deformation moduli for model input will be based on rock-mass classification methods, while the strength properties will be estimated using Hoek-Brown failure criterion for the continuum analysis and Coulomb failure criterion for the discontinuum analysis. Uncertainties will be quantified and their effect on displacement prediction will be evaluated. Furthermore, the uncertainties associated with the joint geometrical information will be considered in displacement prediction for the discontinuum analysis.

Both continuum and discontinuum analyses will be performed at 364, 730, and 1,002 d of heating. Furthermore, failure of elements or blocks will be allowed in the analyses. After failure, the finite elements in the continuum analysis will be assumed to undergo perfectly plastic behavior, while the blocks will break into several pieces in the discontinuum analysis.

3/23

CONTENTS

4/23

FIGURES

5/23

TABLES

ACKNOWLEDGMENTS

This report was prepared to document work performed by the Center for Nuclear Waste Regulatory Analyses (CNWRA) for the U.S. Nuclear Regulatory Commission (NRC) under Contract No. NRC–02–97–009. The activities reported here were performed on behalf of the NRC Office of Nuclear Material Safety and Safeguards, Division of Waste Management. The report is an independent product of the CNWRA and does not necessarily reflect the views or regulatory position of the NRC.

The authors thank B. Dasgupta and B. Sagar for their reviews of this report. The author is thankful to R. Emmot for assisting with the word processing and preparation of the report and to C. Cudd, B. Long, and J. Pryor for editorial reviews.

QUALITY OF DATA, ANALYSES, AND CODE DEVELOPMENT

DATA: No CNWRA-generated original data are contained in this report.

ANALYSES AND CODES: Numerical models presented in this report were developed using computer codes ABAQUS and dda_ct2. The computer code ABAQUS is for continuum analysis of the jointed rock media. This computer code is controlled by the CNWRA software quality assurance procedure (Technical Operating Procedure–018, Development and Control of Scientific and Engineering Software). The computer code dda_ct2 is for discontinuous deformation analysis of jointed rock media. This computer code is currently being developed following the requirements of the CNWRA software quality assurance procedure.

7/23

1 INTRODUCTION

1.1 Background

DECOVALEX (acronym for the **DE**velopment of **CO**upled models and their **VAL**idation against **Ex**periments in nuclear waste isolation) is an international cooperative project to support the development of mathematical models for coupled processes in the geosphere and in thier applications and validation against experiments in the field of nuclear waste isolation. The DECOVALEX project has been designed to increase understanding of coupled thermal-hydrological-mechanical processes as they affect rock-mass responses and radionuclide release and transport from a repository to the biosphere and also to assess how these processes can be described by mathematical models. The DECOVALEX project also attempts to identify contributions of these coupled processes to the overall performance assessment in both near- and far-fields. DECOVALEX includes three phases. DECOVALEX I began in 1991 and was completed in 1995. In this phase, the activities focused on modeling laboratory experiments and benchmark problems. The U.S. Nuclear Regulatory Commission (NRC) was one of the funding members of DECOVALEX I and an active participant. The Center for Nuclear Waste Regulatory Analyses (CNWRA) assisted NRC in performing the analyses. DECOVALEX II started in 1995 and concluded in 1999. This phase focused on using the modeling experience gained during the first phase to simulate experiments conducted in the field. Attention was also given to relate the effects of the thermal-hydrological-mechanical processes to the performance of nuclear waste isolation. The NRC and CNWRA did not participate in this phase of the project. DECOVALEX III began in 1999 and includes four tasks. Task 1 involves modeling the *in situ*, full-scale engineered barriers experiment. Task 2 involves modeling the drift-scale heater test at Yucca Mountain. Task 3 includes three benchmark problems. The first problem presents the implication of thermal-hydrological-mechanical coupling on the near-field performance of a nuclear waste repository. The second problem investigates the effects of upscaling thermal-hydrological-mechanical processes on performance assessment results. The third problem studies the effects of glaciation on rock-mass behavior surrounding a nuclear waste repository. Task 4 attempts to address the issue of applying the effects of thermal-hydrological-mechanical-chemical processes to performance assessment. The NRC, with the assistance of the CNWRA, is actively participating in the DECOVALEX III project. Task 2 is the focus of NRC involvement because this task is most relevant to the high-level waste program in the United States.

1.2 Objective and Scope

As discussed previously, Task 2 of the DECOVALEX III project models the thermal-hydrological-mechanical-chemical behavior of the drift-scale heater test performed at the Exploratory Studies Facility at Yucca Mountain, Nevada. This task includes four subtasks. Subtask 2A focuses on performing thermal-hydrological modeling analyses of the drift-scale heater test to predict the temperature and saturation distribution in the rock during the heating and cooling phases of the test. The outcome of this predictive analysis forms the basis for comparison with the measured temperatures and saturations to validate the models used to represent thermal-hydrological processes. Subtask 2B is related to modeling of rock-mass deformation at various times of the heating and cooling phases of the test. The predicted and measured displacements will be compared to validate the thermal-hydrological-mechanical

models. In this subtask, the predicted temperatures from Subtask 2A will be used for analyses. Subtask 2C also involves thermal-mechanical modeling of the drift-scale heater test. This subtask, however, uses measured temperatures for analysis instead of the predicted ones from Subtask 2A. Subtask 2D includes modeling of thermal-hydrological-chemical processes associated with the drift-scale heater test.

The NRC/CNWRA modeling effort for Task 2 focuses on Subtasks 2A and 2C. Analyses for Subtask 2A have been completed. A report documenting analyses results for the progress on Subtask 2A was submitted to NRC and the Secretariat of the DECOVALEX III project in May 2001 (Green et al., 2001) and is currently being reviewed by the international research teams of the DECOVALEX III project.

On completion of the thermal-hydrological analysis of the drift-scale heater test in Subtask 2A in May 2001, the preliminary analysis for Subtask 2C began late in fiscal year 2001. This report presents the technical approach adopted and a detailed work plan for Subtask 2C. This technical approach has been presented at the DECOVALEX III Annual Workshop in Naantali, Finland, October 22–26, 2001. Specific topics addressed in this report are (i) technical approach, (ii) thermal-mechanical models to be used in the analysis, (iii) work plan, and (iv) schedule. The modeling studies proposed in this report are an important part of the process for assessing and developing confidence on both U.S. Department of Energy models and those models used by NRC to independently evaluate the safety case for the proposed geologic repository at Yucca Mountain.

2 TECHNICAL APPROACH

Two fundamentally different approaches are available for numerically modeling rock mass below ground. The first modeling approach assumes that a rock mass behaves as a continuous material often called the continuum approach. The presence of discontinuities may be accounted for by making various assumptions. It is a common understanding that discontinuities in rock media make rock media softer and weaker. A softer rock deforms more and can be reflected by systematically adjusting rock stiffness parameters. A weaker rock can be modeled by reducing the rock strength parameters. The finite element technique is well-suited for modeling this type of material. The second concept for modeling rock mass is to include discontinuities explicitly into the model, and the discontinuities are modeled by appropriate material and strength properties. This approach is referred to as the discontinuum approach. Discrete element and discontinuous deformation analysis methods are among the techniques currently available and used for direct modeling of discontinuities in the numerical analysis.

In the exercise of Subtask 2C for thermal-mechanical modeling of the drift-scale heater test, both finite element and discontinuous deformation analysis methods will be used. The finite element code to be used for conducting the continuum analysis is ABAQUS. ABAQUS is a commercially available code that has been widely used for modeling geological media. ABAQUS is controlled by the CNWRA software quality assurance procedure (Technical Operating Procedure–018, Development and Control of Scientific and Engineering Software). For conducting discontinuum analysis, a computer code called dda_ct2 will be used. The dda_ct2 code is a modified version of the computer code developed by Shi (1993, 1996, 1998).

The fundamental theory on the finite element method is well-developed and documented in many textbooks. Consequently, this theory will not be presented in this report. The theory of discontinuous deformation analysis, on the other hand, is not well published. It is for this reason that the discontinuous deformation analysis theory is briefly discussed in the following sections. It should be noted that the discontinuous deformation analysis is often known by researchers as DDA, consequently, the term DDA will be used throughout this report.

2.1 Formulation of Discontinuous Deformation Analysis

DDA is suited for investigating fractured rock-mass behavior important to many geotechnical and structural problems. DDA is the block system version of the finite element method. DDA includes a finite element type of mesh where each element represents an isolated block, bounded by preexisting discontinuities (or joints). Although DDA seems to resemble the distinct element method in that it accounts for joint contact behavior, mathematically it parallels finite element method in the following aspects (Shi, 1996):

- DDA establishes its equilibrium equations by minimizing the total potential energy of the system
- DDA uses displacements as unknowns for the simultaneous equations
- Stiffness, mass, and loading matrices of individual blocks are calculated independently and added to the global matrix of the entire system

The blocks simulated in DDA can be of any shape (both convex and concave). An implicit solution algorithm is adopted in the DDA. The large displacements of the blocks are accounted for by the use of a timestep scheme; at the end of each timestep, equilibrium is reached by minimizing the total potential energy and ensuring that contacts on joints are no longer changing contact status, and block geometry is updated. The deformed block geometry, resulting state of stresses, and the status of contacts from the previous timestep are used as the initial condition for the next timestep. A so-called open-close logic scheme is used for determining the status of contacts and will be discussed later.

In the original DDA formulation (Shi, 1993, 1996), it was suggested that a polynomial displacement function could be used to describe the movement of any point in a two-dimensional domain. In developing the computer code for DDA, a first order polynomial displacement function was assumed, so that the stresses and strains within a block in the model were constant. In the first order approximation formulation, the *x*- and *y*-direction displacements, (u, v), at any point (x, y) of a block, can be expressed using six displacement variables (Shi, 1996):

$$\begin{pmatrix} u \\ v \end{pmatrix} = \begin{pmatrix} 1 & 0 & -(y-y_0) & x-x_0 & 0 & \frac{y-y_0}{2} \\ 0 & 1 & x-x_0 & 0 & y-y_0 & \frac{x-x_0}{2} \end{pmatrix} \begin{pmatrix} u_0 \\ v_0 \\ r_0 \\ \varepsilon_x \\ \varepsilon_y \\ \gamma_{xy} \end{pmatrix} \tag{2-1}$$

where

(x_0, y_0)	—	reference point in the block (for convenience, centroid of the block is normally used)
(u_0, v_0)	—	rigid body translation of point (x_0, y_0)
r_0	—	rotation angle of the block with respect to point (x_0, y_0)
ε_x, ε_y, and γ_{xy}	—	normal and shear strains of the block.

Eq. (2-1) can be generalized as

$$\begin{pmatrix} u_i \\ v_i \end{pmatrix} = [W_i][D_i] = \begin{pmatrix} t_{11}^i & t_{12}^i & t_{13}^i & t_{14}^i & t_{15}^i & t_{16}^i \\ t_{21}^i & t_{22}^i & t_{23}^i & t_{24}^i & t_{25}^i & t_{26}^i \end{pmatrix} \begin{pmatrix} d_{1i} \\ d_{2i} \\ d_{3i} \\ d_{4i} \\ d_{5i} \\ d_{6i} \end{pmatrix} \tag{2-2}$$

where the subscript *i* denotes the i^{th} block, $[W_i]$ is the transformation function, and $[D_i]$ contains the variables mentioned earlier.

Hsiung (2001) introduced a more generalized formulation to permit the original DDA computer code to accept any order of polynomial displacement functions. In the generalized formulation, the displacements *(u,v)* at any point *(x,y)* in a block can be represented using the approximation of an n^{th} order polynomial displacement function:

$$u = \sum_{\ell=0}^{n} \sum_{m=0}^{\ell} d_{2\left(m+\sum_{k=1}^{\ell} k\right)+1} x^{\ell-m} y^{m}$$
$$v = \sum_{\ell=0}^{n} \sum_{m=0}^{\ell} d_{2\left(m+\sum_{k=1}^{\ell} k\right)+2} x^{\ell-m} y^{m} \qquad (2\text{-}3)$$

where n is the order, ℓ is an integer from 0 to n, m is an integer from 0 to ℓ, and d_j are the coefficients of the polynomial function. Eq. (2-3) can be expressed as

$$\begin{pmatrix} u \\ v \end{pmatrix} = \left[W_i\right]_{2\times\left(\sum_{\ell=1}^{n+1} 2\ell\right)} \left[D_i\right]_{\left(\sum_{\ell=1}^{n+1} 2\ell\right)\times 1} \qquad (2\text{-}4)$$

where the subscript *i* represents the i^{th} block, $\left[W_i\right]$ is a collection of the $x^{\ell-m}y^{m}$ terms in Eq. (2-3) and a $2 \times \sum_{\ell=1}^{n+1} 2\ell$ matrix, and $\left[D_i\right]$ is the collection of coefficients of the polynomial function, d_j, and a $\sum_{\ell=1}^{n+1} 2\ell \times 1$ matrix.

Assuming that a system contains *N* number of blocks, the total potential energy Π_s of the system has the form

$$\Pi_s = \frac{1}{2}[D_s]^T[K_s][D_s] + [D_s]^T[F_s] + C \qquad (2\text{-}5)$$

where

$$[D_s] = \begin{bmatrix} D_1 \\ D_2 \\ \vdots \\ D_N \end{bmatrix} \qquad (2\text{-}6)$$

is a matrix containing displacement variables of the system,

$$[K_s] = \begin{bmatrix} K_{11} & K_{12} & \cdots & K_{1N} \\ K_{21} & K_{22} & \cdots & K_{2N} \\ \vdots & \vdots & \ddots & \vdots \\ K_{N1} & \cdots & \cdots & K_{NN} \end{bmatrix} \tag{2-7}$$

is the system stiffness matrix (Shi, 1996), and C is the energy produced by friction forces between blocks (along the contacts). If an n^{th} order displacement function is chosen, there are $\sum_{\ell=1}^{n+1} 2\ell$ displacement variables/unknowns for each block in the system. As a result, each element itself in matrices $[D_s]$ and $[F_s]$ is a $1 \times \sum_{\ell=1}^{n+1} 2\ell$ matrix and each element in $[K_s]$ is a $\sum_{\ell=1}^{n+1} 2\ell \times \sum_{\ell=1}^{n+1} 2\ell$ matrix.

By minimizing the total potential energy of the system, a set of simultaneous equations can be obtained

$$[K_s][D_s] = [F_s] \tag{2-8}$$

The stiffness matrix $[K_s]$ and the force matrix $[F_s]$ take the contribution from the elastic strains, displacement and load boundary conditions, initial stresses, force inertia, thermal stresses, and contacts between blocks. The general forms of the formulations for these contributions for the n^{th} order approximation are similar to those for the first order approximation except that appropriate transformation function approximation should be used. Some of the formulations are presented in the following sections.

2.1.1 Block Stiffness Matrix

The strain energy Π_e for block i can be expressed

$$\Pi_e = \iint \frac{1}{2}[\varepsilon_i][\sigma_i]\, dxdy \tag{2-9}$$

where σ_i is the stress matrix and ε_i is the strain matrix of block i. The stress-strain relationship can be presented as

$$[\sigma_i] = [E_i][\varepsilon_i] \tag{2-10}$$

For a plane stress condition

$$[E_i] = \frac{E}{1-\nu}\begin{bmatrix} 1 & \nu & 0 \\ \nu & 1 & 0 \\ 0 & 0 & \frac{1-\nu}{2} \end{bmatrix} \tag{2-11}$$

For a plane strain condition

$$[E_i] = \frac{E(1-\nu)}{1-\nu}\begin{bmatrix} 1 & \frac{\nu}{1-\nu} & 0 \\ \frac{\nu}{1-\nu} & 1 & 0 \\ 0 & 0 & \frac{1-2\nu}{2(1-\nu)} \end{bmatrix} \tag{2-12}$$

where E is Young's Modulus, v is Poisson's ratio, and the strains $[\varepsilon_i]$ can be determined by

$$\begin{bmatrix} \varepsilon_x \\ \varepsilon_y \\ \gamma_{xy} \end{bmatrix} = \begin{bmatrix} \frac{\partial u}{\partial x} \\ \frac{\partial v}{\partial y} \\ \frac{\partial u}{\partial y} + \frac{\partial v}{\partial x} \end{bmatrix} = [B_i][D_i] \tag{2-13}$$

The $[B_i]$ matrix can be obtained by taking the derivative of the elements in the transformation function $[W_i]$ with respect to appropriate variables indicated in Eq. (2-13) and is a $3 \times \sum_{\ell=1}^{n+1} \ell$ matrix. With Eq. (2-13), Eq. (2-10) can be expressed by

$$[\sigma_i] = [E_i][B_i][D_i] \tag{2-14}$$

Substituting Eqs. (2-13) and (2-14) into Eq. (2-9), the strain energy of block i will be

$$\Pi_e = \iint \frac{1}{2}[D_i]^T[B_i]^T[E_i][B_i][D_i]\,dx\,dy \tag{2-15}$$

The contribution of the stiffness matrix to the overall stiffness matrix from block i is determined by minimizing Eq. (2-15)

$$[K_{ii}] = \iint [B_i]^T[E_i][B_i]\,dx\,dy \tag{2-16}$$

It should be noted that the elements in $[B_i]$ matrix contain $x^{n_1}y^{n_2}$ terms, where n_1 and n_2 are integers equal to or greater than zero. Consequently, integration of Eq. (2-16) is not straightforward. Shi (1994) presented the analytical solutions that make integration of any polynomial term possible. Chen and Ohnishi (1999) further reduced the solutions to a more manageable form.

2.1.2 Initial Stress

The initial stresses $\left[\sigma_i^0\right]$ in block *i* at the beginning of a timestep are

$$\left[\sigma_i^0\right] = \left[E_i\right]\left[\varepsilon_i^0\right] = \left[E_i\right]\left[B_i\right]\left[D_i^0\right] \tag{2-17}$$

The potential energy Π_{σ^0} for the initial stresses in block *i* is

$$\begin{aligned}\Pi_{\sigma^0} &= \iint\left[\varepsilon_i\right]\left[\sigma_i^0\right]dxdy \\ &= \iint\left[D_i\right]^T\left[B_i\right]^T\left[E_i\right]\left[B_i\right]\left[D_i^0\right]dxdy\end{aligned} \tag{2-18}$$

The contribution of the initial stresses in block *i* to the overall force matrix is calculated by minimizing Eq. (2-18) and is expressed as

$$\left[F_i\right] = -\iint\left[B_i\right]^T\left[E_i\right]\left[B_i\right]dxdy\left[D_i^0\right] \tag{2-19}$$

2.1.3 Thermal Stress

The thermal stresses $\left[\Delta\sigma_i^t\right]$ in block *i* for plane stress conditions can be expressed as

$$\left[\Delta\sigma_i^t\right] = \frac{E}{1-\nu}\alpha\Delta T \tag{2-20}$$

and for plane strain conditions is (Itasca Consulting Group, Inc., 2000)

$$\left[\Delta\sigma_i^t\right] = \frac{E}{1-2\nu}\alpha\Delta T \tag{2-21}$$

The potential energy Π_{σ^t} for these thermal stresses in block *i* may be expressed by the following equation

$$\begin{aligned}\Pi_{\sigma^t} &= \iint [\varepsilon_i][\sigma_i^t]\,dxdy \\ &= \iint [D_i]^T [B_i]^T [E_i][B_i][D_i^t]\,dxdy\end{aligned} \tag{2-22}$$

The contribution of the thermal stresses in block *i* to the overall force matrix is calculated by minimizing Eq. (2-22) and is expressed as

$$[F_i] = -\iint [B_i]^T [E_i][B_i]\,dxdy\,[D_i^t] \tag{2-23}$$

2.1.4 Body Force

For a constant body force (f_x, f_y) in block *i*, the associated potential energy Π_b of a constant body force is

$$\Pi_b = -\iint \begin{bmatrix} u & v \end{bmatrix} \begin{bmatrix} f_x \\ f_y \end{bmatrix} dxdy \tag{2-24}$$

Substituting Eq. (2-4) into Eq. (2-24), the potential energy equation can be rewritten as

$$\Pi_b = -\iint [D_i]^T [W_i]^T \begin{bmatrix} f_x \\ f_y \end{bmatrix} dxdy \tag{2-25}$$

Minimizing Eq. (2-25), the contribution of the body force in block *i* to the overall force matrix is

$$[F_i] = \iint [W_i]^T dxdy \begin{bmatrix} f_x \\ f_y \end{bmatrix} \tag{2-26}$$

2.1.5 Displacement Constraints

As a boundary condition, specific points in a system may be fixed to prevent movement. This constraint can be achieved by applying stiff springs. Assuming the resulting residual displacement of the fixed point in block *i* after a timestep is (*u*, *v*), and two springs with a stiffness of *p* are applied to this point (one is along the *x* direction and the other, *y* direction), the spring forces $\begin{bmatrix} f_x^s & f_y^s \end{bmatrix}$ at the fixed point are

$$\begin{bmatrix} f_x^s \\ f_y^s \end{bmatrix} = \begin{bmatrix} -pu \\ -pv \end{bmatrix} \tag{2-27}$$

It should be noted that the magnitude of the residual displacement depends on the spring stiffness applied. The larger the spring stiffness is, the smaller the residual displacement. The strain energy Π_s associated with the springs is

$$\begin{aligned}\Pi_s &= \frac{p}{2}\begin{pmatrix} u & v \end{pmatrix}\begin{pmatrix} u \\ v \end{pmatrix} \\ &= \frac{p}{2}[D_i]^T[W_i]^T[W_i][D_i]\end{aligned} \tag{2-28}$$

The contribution to the system stiffness matrix from the fixed point can be obtained by minimizing Eq. (2-28)

$$[K_{ii}] = p[W_i]^T[W_i] \tag{2-29}$$

2.1.6 Inertia Force

Because the DDA method is based on dynamic approach, inertia force plays an important role in block motion. When a block moves in dynamic mode, the initial velocity of this block at the beginning of a timestep should be equal to its velocity at the end of the previous timestep. Newton's second law of motion is used to regulate the block movement. For the time-dependent displacement (u, v) of any point in the i^{th} block, the associated inertia force per unit area (f_x, f_y) is

$$\begin{pmatrix} f_x \\ f_y \end{pmatrix} = -M\frac{\partial^2}{\partial t^2}\begin{bmatrix} u(t) \\ v(t) \end{bmatrix} \tag{2-30}$$

where M is the mass per unit area. The potential energy Π_I for the inertia force can be written as follows:

$$\Pi_I = \iint M\begin{pmatrix} u & v \end{pmatrix}\begin{bmatrix} \frac{\partial^2 u(t)}{\partial t^2} \\ \frac{\partial^2 v(t)}{\partial t^2} \end{bmatrix} dxdy \tag{2-31}$$

Eq. (2-31) can be expressed as displacement variables and transformation function

$$\Pi_I = \iint M[D_i]^T[W_i]^T[W_i]\frac{\partial D_i(t)}{\partial t^2}dxdy \tag{2-32}$$

Expanding the partial derivative term in Eq. (2-32) based on the Taylor series using the timestep increment Δ and omitting the higher order terms, the partial derivative term can be shown as

$$\frac{\partial^2 D_i(t)}{\partial t^2} = \frac{2}{\Delta^2}[D_i] - \frac{2}{\Delta}\frac{\partial D_i(t)}{\partial t} \tag{2-33}$$

where $\frac{\partial D_i(t)}{\partial t}$ is the velocity V_0 at the end of the previous timestep. Minimizing Eq. (2-33), the contribution of the stiffness matrix to the overall stiffness matrix from block *i* from the inertia force is

$$[K_{ii}] = \frac{2M}{\Delta^2}[W_i]^T[W_i]\,dxdy \tag{2-34}$$

and the force matrix contribution to the overall force matrix is

$$[F_i] = \frac{2M}{\Delta}\left(\iint [W_i]^T[W_i]\,dxdy\right)[V_0] \tag{2-35}$$

2.2 Contact Judging

To model a blocky system, a complete solution has to satisfy both equilibrium and compatibility conditions (Ma, 1999). The DDA uses an open-close iteration criterion to fulfill the compatibility conditions between blocks by solving a set of algebraic inequalities through iterations within a given timestep (Shi, 1996). The open-close iteration process continues until no tension or penetration occurs at all conditions of contact modes before the calculation proceeds to the next timestep. Based on natural contact phenomena, three basic contact modes can be identified: open, sliding, and locking.

Assume point P_1 has the coordinates (x_1, y_1), and line $\overline{P_2P_3}$ has the coordinates (x_2, y_2), and (x_3, y_3) at the two end points (solid lines in Figure 2-1). After deformation, P_1 and $\overline{P_2P_3}$ changed their positions to broken lines as shown in Figure 2-1. The contact condition of P_1versus line $\overline{P_2P_3}$ can be described by the inequality (Shi, 1996)

$$\Delta = \begin{vmatrix} 1 & x_1 + u_1 & y_1 + v_1 \\ 1 & x_2 + u_2 & y_2 + v_2 \\ 1 & x_3 + u_3 & y_3 + u_3 \end{vmatrix} < 0 \tag{2-36}$$

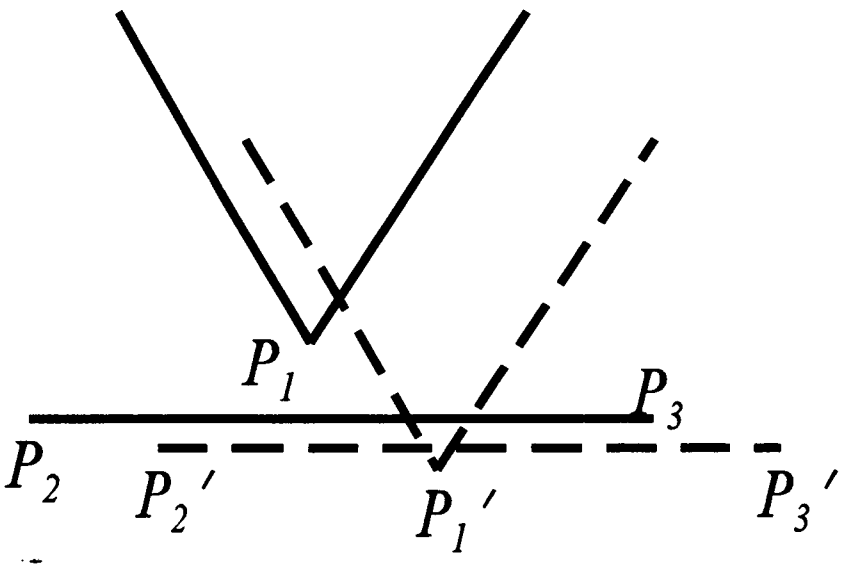

Figure 2-1. Contact Determination

where Δ is the determinant. When Δ is positive, P_1 has no contact with $\overline{P_2P_3}$. Otherwise, P_1 is in contact with $\overline{P_2P_3}$. The distance d between P_1 and $\overline{P_2P_3}$ after deformation can be approximated assuming small deformation using

$$d = \frac{\Delta}{\sqrt{(x_2 - x_3)^2 + (y_2 - y_3)^2}} \tag{2-37}$$

In DDA, Coulomb's Law is applied to assess the contact conditions between blocks. At every iteration, each contact is evaluated to determine if

- The normal contact force at the contact is greater than or equal to the contact tensile strength
- The shear contact force is smaller than the contact shear strength multiplied by the half length of the block edge where this contact is located, when the normal contact force is compressive
- The shear contact force is greater than or equal to the contact shear strength multiplied by the half length of the block edge where this contact is located, when the normal contact force is compressive

If the first condition is satisfied, the contact is judged as open and no normal spring is applied. When the second condition is met, the contact is essentially locked such that no sliding between point P_1 and line $\overline{P_2P_3}$ has occurred. In this condition, both normal and shear stiffnesses are simulated using normal and shear springs at the contact. If the third condition is satisfied, P_1 slides along $\overline{P_2P_3}$; a normal spring is added and a pair of friction forces at the contact are added to the system force matrix $[F_s]$. The contribution of the added contact springs should be included in the system stiffness matrix $[K_s]$ to account for the kinematics between blocks in the system. Details regarding how to determine the contribution of joint contact to the system force and stiffness matrices can be found elsewhere (Shi, 1993, 1996).

14/23

3 WORK PLAN FOR THERMAL-MECHANICAL MODELING OF DRIFT-SCALE HEATER TEST

The drift-scale heater test facility is located in the Topopah Spring middle nonlithophysal zone (CRWMS M&O, 1997a). The Topopah Spring middle nonlithophysal zone is approximately 30–40 m [98.4–131.2 ft] thick at the location of the drift-scale test area. This zone is overlain by the Topopah Spring upper lithophysal and underlain by the Topopah Spring lower lithophysal zones. Figure 3-1 shows a generalized stratigraphic column including expanded lithologic information from ground surface to below Calico Hills formation for the proposed repository.[1]

The drift-scale heater test block was characterized prior to the onset of heating. The characterization includes geologic mapping, local geology, rock-mass classification, and some geotechnical data. Figure 3-2 shows a plane view schematic of the drift-scale heater test region and associated access. The heater drift is about 5 m [16.4 ft] in diameter and 47.5-m [155.8-ft] long and is closed at the east end by a thermal bulkhead. Approximately 12 m [139.4 ft] of the heated drift, from the west end, is lined with a cast-in-place concrete liner. A concrete invert was poured along the entire floor of the heated drift. Eight 20-mm [0.79-in] thermal expansion joints were cast into the invert at a nominal spacing of 6 m [19.7 ft]. Thermal sources for the heated drift consist of 9 canister heaters, placed end to end on the concrete inverts of the heated drift and 50 wing heaters (25 on either side) placed in horizontal boreholes drilled into the sidewalls of the heated drift about 0.25 m [0.8 ft] below the springline. Locations of the wing heaters around the heated drift can be found in a report prepared by CRWMS M&O (1997b). The wing heaters are spaced 1.83 m [6 ft] apart. Each wing heater has two segments {5 m long [16.4 ft]} with a larger power output from the outer segment. The inner wing heater segment is separated from the heater drift by 1.5 m [4.9 ft].

Temperatures are measured at approximately 2,662 locations within the drift-scale heater test block. Temperature measurements in the rock and wing heaters were used in developing the temperature distributions in the rock at intervals of 2 d. The dimensions of the block used for the development of temperature distribution are 70 m [229.7 ft] wide in the x-direction, 60 m [196.8 ft] long in the y-direction (axis along the heated drift), and 70 m [229.7 ft] high in the z-direction. The center of the block is located at the center of the heated drift approximately 25 m [82 ft] from the thermal bulkhead. Ambient temperatures {approximately 24 °C [75 °F]} were applied to the boundaries of the block to develop temperature distribution. The temperature data were generated at intervals of 1 m [3.3 ft] along all three directions. In the process of developing temperature data, if a resulting temperature value was less than 20 °C [68 °F], a value of 20 °C [68 °F] was assigned. This value is slightly lower than the ambient temperature. Figure 3-3 shows the contours of the temperature distribution on a vertical cross section at 23 m [75.5 ft] from the thermal bulkhead of the heated drift after 1,002 d of heating.

The temperature distribution data generated from the measured temperatures are provided to the research teams involved in the modeling effort of Task 2C of the DECOVALEX III project. The NRC/CNWRA research team effort to accomplish Task 2C includes four major activities: (i) development of numerical models, (ii) compilation of material properties input, (iii) production of numerical analyses, and (iv) preparation of the report.

---

[1]This information is provided by the technical monitor research team for Task 2 of the DECOVALEX III project.

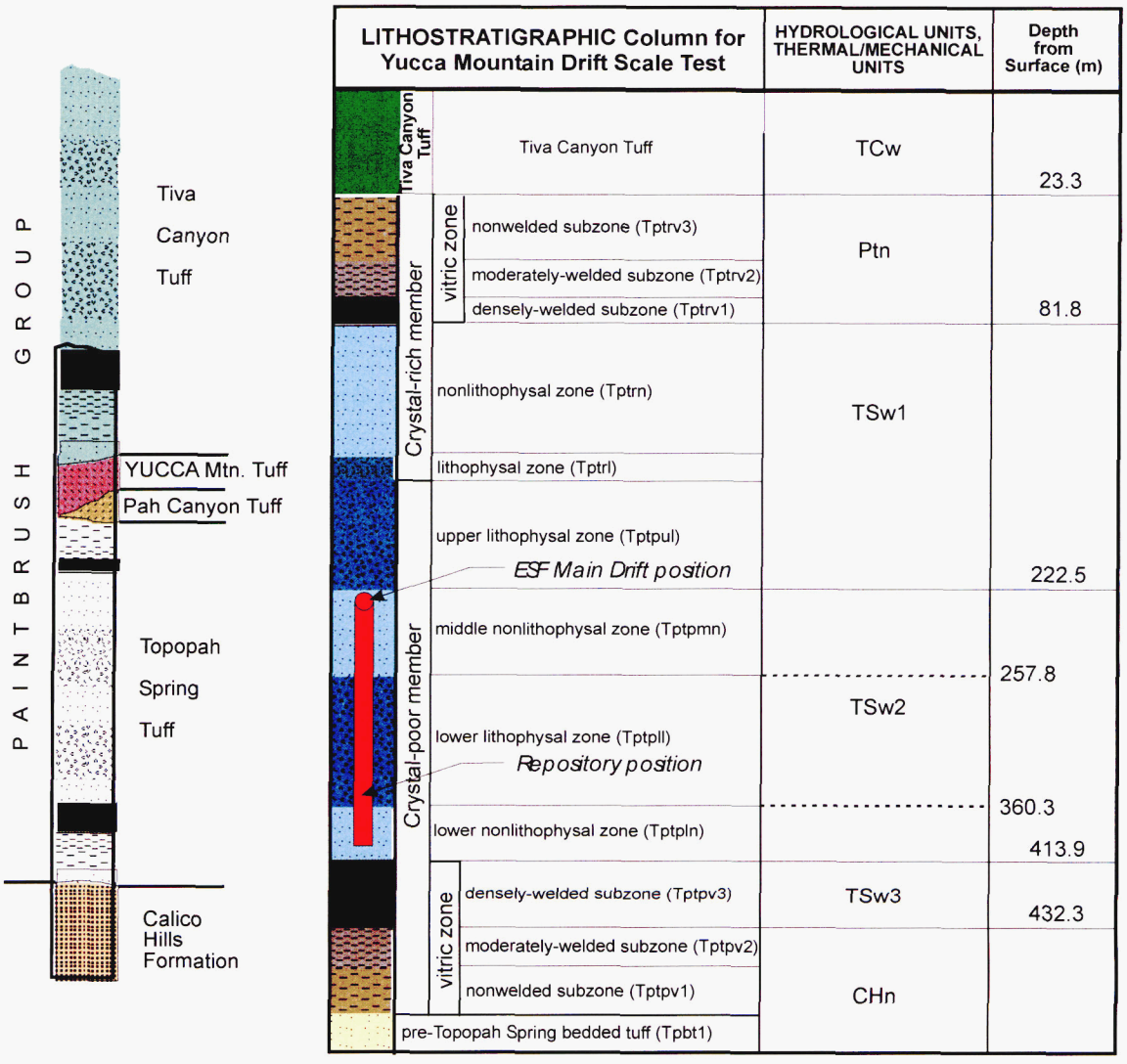

Figure 3-1. Stratigraphic Data for Drift-Scale Heater Test

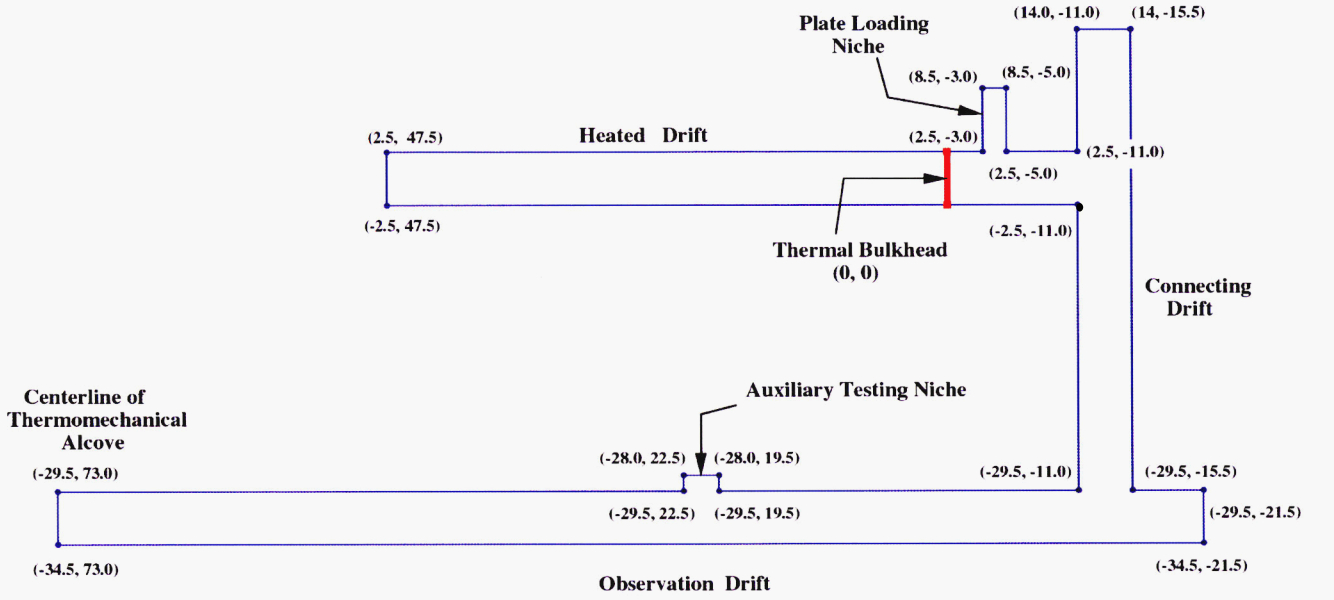

Notes:
1. X and Y coordinates are given in meters.
2. Z coordinates (vertical) are not included.
3. Only key locations are provided.
4. Coordinates are based on design with the following as-builts tolerances:
   Horizontal alignment = - 0 to + 0.5m
   All other = - 0 to + 0.3m

Figure 3-2. Plan View Schematic of the Primary Components of the Drift-Scale Heater Test Region

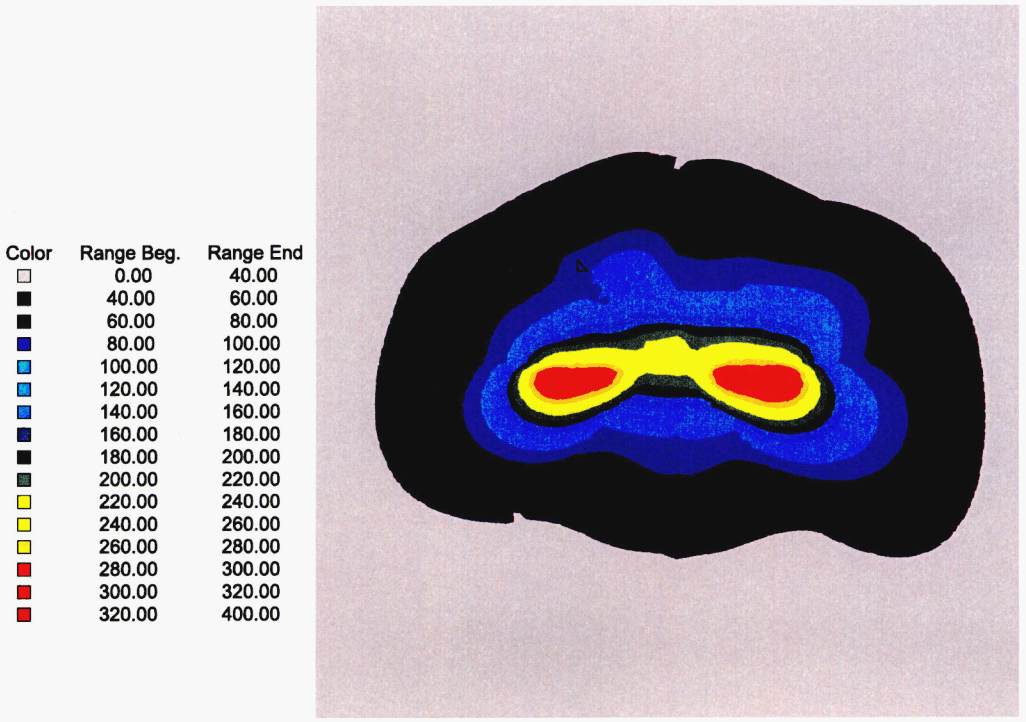

Figure 3-3. Temperature Contour, 23 m [75.5 ft] from the Thermal Bulkhead after 1,002 d of Heating

3.1 Development of Numerical Models

As discussed in Section 2, both continuum and discontinuum analyses will be conducted in this study to predict thermal effects on rock-mass deformation. The two-dimensional numerical models will simulate a plane strain condition. A vertical cross section, 21 m [68.9 ft] from the thermal bulkhead, will be taken to develop the numerical model. This cross section coincides with four multiple position extensometers used for displacement measurements. The models used by both approaches will have the same dimension {200 m [656 ft] wide and tall} with a 5-m [16.4-ft] diameter drift in the middle of the model domain. Fixed horizontal displacement boundaries will be applied to the sides and a fixed vertical displacement boundary to the bottom of the model. A constant stress boundary will be applied to the top of the model to simulate the remaining overburden. Initial stresses consistent with overburden depth will be applied as an initial condition. The thermal load will be calculated based on the temperature distribution at 21 m [68.9 ft] from the thermal bulkhead coinciding with the location of numerical models.

Figure 3-4 gives the schematic drawing of the model domain. Also shown in the figure are points to be included in the model for displacement prediction. These points coincide with the anchor points of the four multiple position extensometers located at the same cross section. For these extensometers, two are vertically oriented (one in the crown and one in the invert), and the remaining two are inclined at approximately 30° to the vertical extensometer on either side of the vertical extensometer. The displacements at these points are necessary for comparison with the measured values.

Because of the size of the model domain currently being considered, the numerical models will include three generalized lithologic zones: Topopah Spring upper lithophysal zone on the top, Topopah Spring middle nonlithophysal zone in the middle, and Topopah Spring lower lithophysal zone on the bottom. The development of finite element models for continuum analysis to include these three zones should be relatively straightforward because the model geometry to be developed is relatively simple. The development of finite element models in this activity will focus on the close vicinity of the heated drift with relatively smaller size of elements. The size of the elements will be scaled up gradually because these elements are located farther from the area of interest. Effort may also be made in this activity to ensure the points at which displacement predictions are required coincide with the physical nodes of the finite elements so that displacements for these points can be obtained directly from the modeling results without interpolation.

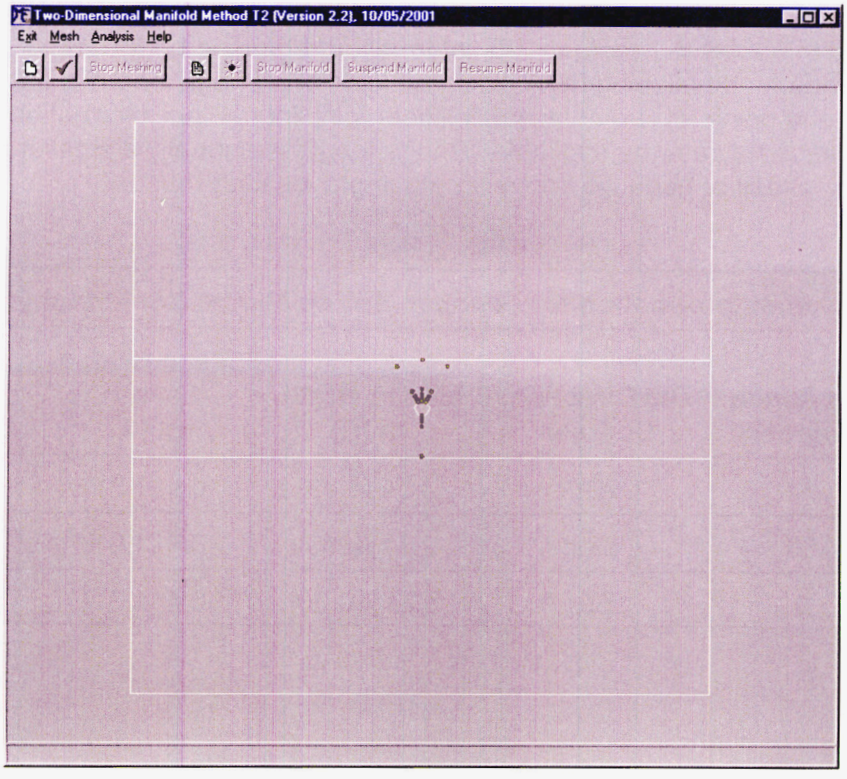

Figure 3-4. Model Domain Schematic

Development of numerical models for DDA for this study will require joint geometrical information for the three lithologic zones mentioned in the previous paragraph. The joint geometrical information required includes orientation, spacing, and length as a minimum. Because the joint information specific to the heated drift is not readily available, the joint information developed from the geological mapping data collected from the Exploratory Studies Facility will be used in this activity as a basis to generate DDA block models. The joint geometrical information for the three lithologic zones presented in Tables 3-1 through 3-3 is estimated from two reports prepared by CRWMS M&O (2000a,b).

Because of the relatively large dimension of the model domain and the large number of small size blocks, using the joint information presented in Tables 3-1 through 3-3 may result in a DDA block model too complicated to conduct the analysis effectively. As a result, this information needs to be adjusted to reduce the number of rock blocks formed for DDA analysis to a manageable manner. For this study, joint spacings and joint lengths for the three lithologic zones will be scaled up. Suggested scaled joint spacing and joint length values are listed in Tables 3-4 through 3-6. Effort will also be made to merge blocks that are extremely small compared to the average block size of the model with the neighboring blocks to avoid numerical instability problems. Further examination of the scaling will be made in this activity to determine a reasonable scaling factor such that analysis can be performed effectively with acceptable run time and free from numerical instability. It should be noted that joint dips and dip directions for the three lithologic zones will not be changed so that a comparable joint pattern can be maintained. Figure 3-5 shows a typical DDA block model developed using the joint information listed in Tables 3-4 through 3-6.

As can be noticed in Tables 3-1 through 3-6, information regarding bridge length is listed. This information is unique for developing DDA block models. The bridge length is defined as the gap between the end points of two adjacent collinear joint lines. This information is assumed for this study because no data are available. Bridge length is normally a smaller value relative to the joint length. Small or negative bridge length improves the probability of forming blocks of reasonable size.

Table 3-1. Joint Information for Topopah Spring Middle Nonlithophysal Zone

Joint Set Number	Dip Angle, Degrees	Dip Direction, Degrees	Mean Length, m [ft]	Mean Bridge Length, m [ft]	Mean Spacing, m [ft]
1	84	221	2.54 [8.33]	0.4 [1.31]	0.60 [1.97]
2	83	299	2.71 [8.89]	0.4 [1.31]	1.92 [6.30]
3	9	59	3.23 [10.60]	0.4 [1.31]	0.56 [1.84]

17/23

Table 3-2. Joint Information for Topopah Spring Lower Lithophysal Zone					
Joint Set Number	Dip Angle, Degrees	Dip Direction, Degrees	Mean Length, m [ft]	Mean Bridge Length, m [ft]	Mean Spacing, m [ft]
1	82	235	4.56 [14.96]	-1.0 [-3.28]	3.47 [11.38]
2	79	270	4.02 [13.19]	-1.0 [-3.28]	4.05 [13.29]
3	5	45	7.36 [24.15]	-1.0 [-3.28]	2.94 [9.65]

Table 3-3. Joint Information for Topopah Spring Upper Lithophysal Zone					
Joint Set Number	Dip Angle, Degrees	Dip Direction, Degrees	Mean Length, m [ft]	Mean Bridge Length, m [ft]	Mean Spacing, m [ft]
1	82	288	3.29 [10.79]	-1.0 [-3.28]	3.76 [12.34]
2	82	229	2.88 [9.45]	-1.0 [-3.28]	3.76 [12.34]
3	14	40	5.16 [16.93]	-1.0 [-3.28]	3.21 [10.53]

Table 3-4. Adjusted Joint Information for Topopah Spring Middle Nonlithophysal Zone for Modeling Use					
Joint Set Number	Dip Angle, Degrees	Dip Direction, Degrees	Mean Length, m [ft]	Mean Bridge Length, m [ft]	Mean Spacing, m [ft]
1	84	221	10.16 [33.33]	0.4 [1.31]	2.40 [7.87]
2	83	299	10.84 [35.56]	0.4 [1.31]	7.68 [25.20]
3	9	59	12.94 [42.45]	0.4 [1.31]	2.24 [7.35]

Table 3-5. Adjusted Joint Information for Topopah Spring Lower Lithophysal Zone for Modeling Use					
Joint Set Number	Dip Angle, Degrees	Dip Direction, Degrees	Mean Length, m [ft]	Mean Bridge Length, m [ft]	Mean Spacing, m [ft]
1	82	235	22.8 [74.80]	-1.0 [-3.28]	5.21 [17.09]
2	79	270	20.10 [65.94]	-1.0 [-3.28]	6.08 [19.95]
3	5	45	31.80 [104.33]	-1.0 [-3.28]	4.41 [14.47]

Table 3-6. Adjusted Joint Information for Topopah Spring Upper Lithophysal Zone for Modeling Use					
Joint Set Number	Dip Angle, Degrees	Dip Direction, Degrees	Mean Length, m [ft]	Mean Bridge Length, m [ft]	Mean Spacing, m [ft]
1	82	288	16.45 [53.97]	-1.0 [-3.28]	5.63 [18.47]
2	82	229	14.90 [48.88]	-1.0 [-3.28]	5.63 [18.47]
3	14	40	25.80 [84.64]	-1.0 [-3.28]	4.82 [15.81]

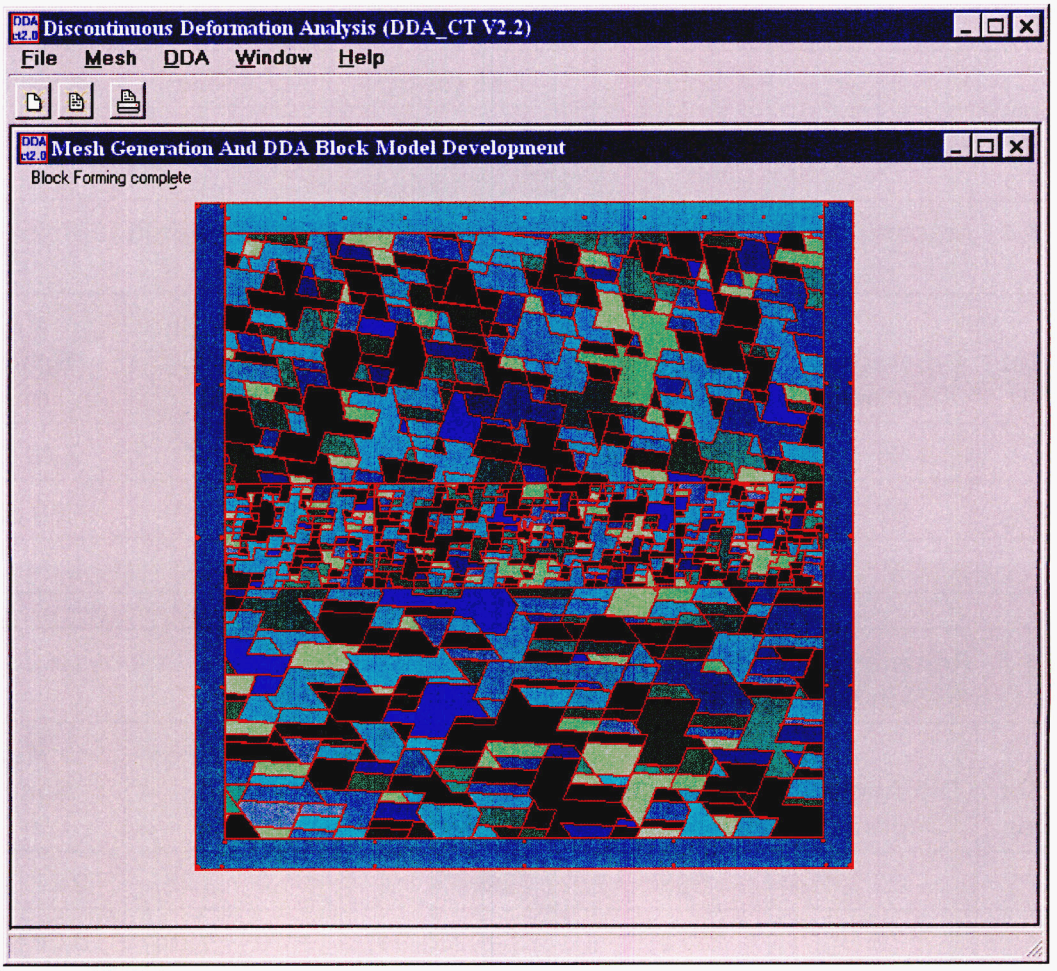

Figure 3-5. Discontinuous Deformation Analysis Block Model 1

3.2 Compilation of Material Properties Input

Material properties needed for both continuum and discontinuum analyses to be performed in this study include (i) rock-mass deformation modulus, (ii) Poisson's ratio, and (iii) strength properties. Additional material properties necessary for discontinuum analysis include (i) joint normal and shear stiffnesses and (ii) joint cohesion and friction angle. The objectives of this activity involve collecting and compiling input information for modeling use.

3.2.1 *In-Situ* Deformation Moduli

The *in-situ* deformation modulus of a rock mass is an important parameter in any form of numerical analysis and in the interpretation of monitored deformation around the heated drift. The intact rock Young's moduli, along with Poisson's ratios and bulk densities, for the three lithologic zones are listed in Table 3-7. As discussed in Section 1, the presence of discontinuities in rock media tends to soften and weaken a rock medium. Therefore, the deformation modulus of a rock mass could be substantially different from that of the intact rocks that form the rock mass. The extent of difference in deformation modules depends on the intensity and the surface properties of joints present in the host rock. A reasonable approach to determine rock-mass deformation modulus is to conduct tests in the field. This approach, however, is often difficult to perform and is expensive. Attempts have been made to develop methods for estimating its value, based on rock-mass classifications. The two most widely used rock-mass classifications are the RMR (Bieniawski, 1976, 1989) and the Q (Barton et al., 1974). Both methods rely heavily on joint information.

Table 3-7. Rock Block Material Properties [CRWMS M&O (1997c)]

	Upper Lithophysal Zone	Middle Nonlithophysal Zone	Lower Lithophysal Zone
Bulk Density, kg/m^3 [lb/ft^3]	2,160±80 [134.8±5.0]	2,250±70 [140.5±4.4]	2,250±60 [140.5±3.7]
Young's Modulus, Gpa [10^6 psi]	20.36±6.75 [2.95±0.98]	32.93±5.47 [4.77±0.79]	27.54±7.49 [3.99±1.09]
Poisson's Ratio	0.23±0.07	0.21±0.03	0.21±0.06

It should be noted, however, large uncertainties are associated with the characterization of joint intensity and joint properties. Consequently, determination of rock-mass deformation modulus by taking into consideration the presence of joints will similarly involve large uncertainties. As part of this subactivity, both rock-mass classification methods will be used to derive rock-mass deformation modulus. Attempts will be made to quantify the uncertainties. The uncertainties may be evaluated to estimate their effects on displacement prediction in the Task 2C, activity (iii): Numerical Analyses.

It is recognized that the deformation modulus for rock blocks in a discontinuum analysis may be different from that for elements in a continuum analysis because at least a portion of the joints in the rock mass is modeled explicitly. It is reasonable not to include the effects of these

explicitly modeled joints from the estimation of the rock-mass deformation modulus. Otherwise, these effects tend to be double counted, resulting in an overprediction of displacements. No acceptable procedure is available for this exercise. Consequently, overprediction may be an acceptable alternative (i.e., use the rock-mass deformation modulus in the discontinuum analysis).

3.2.2 Strength Properties

Another important parameter to support numerical analysis of rock-mass behavior is strength properties. These properties are equally if not more difficult to determine than the rock-mass deformation modulus. In this study, the Hoek-Brown failure criterion will be used in the continuum analysis to judge failure of finite elements. The procedure outlined by Hoek and Brown (1997) will be followed to estimate the related strength properties. Previous work conducted by the CNWRA on rock-mass strength properties for the Topopah Spring middle nonlithophysal zone (Ofoegbu, 2000) will be considered in this subactivity.

While applying this failure criterion, particular attention will be made to its applicability to the rock masses being considered. Hoek, et al. (1995) indicate,"the Hoek-Brown failure criterion is only applicable to intact rock or to heavily jointed rock masses which [sic] can be considered homogeneous and isotropic." In other words, the use of this failure criterion is not appropriate for conditions in which an individual joint set has a dominant influence on the behavior of the rock mass even in extreme cases (Hoek, et al., 1995).

For discontinuum analysis, the Mohr-Coulomb failure criterion may be used to assess potential failure of rock blocks and the corresponding strength parameters will be derived, in this subactivity, from the Hoek-Brown failure criterion (Hoek and Brown, 1997). As an alternative, the Hoek-Brown failure criterion could be coded into the dda_ct2 computer program and used as the failure criterion to assess block failure. This option is being considered.

A concern similar to that discussed in the last paragraph of Section 3.2.1 is equally applicable to the determination of strength properties for the blocks of discontinuum analysis. Unless a viable alternative can be found, rock-mass strength properties will be assumed for the blocks.

3.2.3 Joint Stiffness and Strength Properties

The primary objective of this subactivity is to collect and develop, if necessary, joint stiffness and strength properties for the three lithologic zones for discontinuum modeling. Limited test results of joints related to the Topopah Spring rock unit are presented in a report prepared by CRWMS M&O (1997c). These joint properties along with the test results on the Apache Leap tuff joints, obtained from an early CNWRA study sponsored by the NRC Office of Research (Hsiung, et al., 1994), will be analyzed together in this subactivity to develop reasonable joint properties for the study.

3.3 Numerical Modeling

Thermal-mechanical modeling of the drift-scale heater test for Subtask 2C of the DECOVALEX III project will be performed using both the finite element and DDA methods. Planned work related to this activity is discussed in the following subsections.

3.3.1 Continuum Analyses

In this subactivity, the finite element computer code ABAQUS will be used to conduct the continuum analysis. The material and strength properties obtained from Subsections 3.2.1 and 3.2.2, along with the coefficients of thermal expansion and the temperature distribution data, will be used as input for the analysis.

The analysis will be performed at three discrete heating times: 364, 730, and 1,002 d. At each discrete time, the state of stresses for the overall model and the displacements at predetermined locations will be assessed. Failure of finite elements is allowed, and the failed elements are assumed to exhibit perfectly plastic behavior.

If time permits, the effects of uncertainties associated with the rock-mass deformation modulus and the strength properties will be evaluated and quantified in the analysis. The primary focus will be the effects of the property uncertainties related to the Topopah Spring middle nonlithophysal zone.

3.3.2 Discontinuum Analyses

In this subactivity, the computer code dda_ct2 will be used to conduct the discontinuum analysis. The material and strength properties obtained from Subsections 3.2.1, 3.2.2, and 3.2.3, along with the coefficients of thermal expansion and the temperature distribution data, will be used as input for the analysis.

Similar to the continuum analysis, the DDA will be performed at three discrete heating times: 364, 730, and 1,002 d. At each discrete time, the state of stresses for the overall model and the displacements at specific points will be assessed. The dda_ct2 computer code to be used in this study permits rock blocks to break if the failure condition is met. As discussed previously, a Mohr-Coulomb failure criterion is available for judging block failure. When the block is failed, it will be broken into two or four subblocks, depending on the type of failure experienced. For shear failure, the block will break into four pieces and for tensile failure, two pieces .

Furthermore, to account for variations and uncertainties associated with the joint geometrical information, a Monte Carlo technique will be adopted to generate sample joint spacings and joint lengths. Note that each sample generated is an equally likely realization of joints that honor the information used. In generating these realizations, the joint spacing, length, and bridge length will be assumed uniformly distributed and varied ±30 percent around the mean values of the respective parameters. The fracture geometry analysis report prepared by CRWMS M&O (2000b) shows that the joint spacings and trace lengths for the four Topopah Spring lithologic zones are mostly lognormally distributed, and some are exponentially distributed. Depending on the lower and upper limits used to constrain sampling, the assumption of uniform distribution used in this analysis could potentially underestimate the maximum block size but overestimate the number of relatively large blocks available. This potential overestimation or underestimation may not be of significance in that the joint spacings and joint lengths are scaled up already in this study to reduce unnecessary complexity of the problem. By the same token, uncertainties in joint dip angle and dip direction will not be considered in the analyses planned in this study to avoid producing overly complicated DDA

block models. Figures 3-6 and 3-7 show two example realizations of joint distributions generated stochastically for constructing DDA block models. These two realizations used the same joint information listed in Tables 3-4 through 3-6.

The joint distribution realizations similar to those in Figures 3-6 and 3-7 can be further processed using a preprocessor with the dda_ct2 computer code to form blocks for DDA modeling. This preprocessor uses a tree-cutting procedure to remove joints or portions of joints that do not contribute to the formation of blocks because DDA ignores those joint segments that do not belong to a block edge. The detailed discussion on the tree-cutting procedure is in Shi (1996). Figures 3-5 and 3-8 show typical DDA block models. Notice that the rock blocks formed shown in the figures contain many different shapes with any number of vertices. These shapes are often complex. Many of the blocks are concave. It can also be observed that the block sizes and locations of blocks associated with the two models vary. It should be noted that the ultimate shapes and locations of the blocks are controlled by the persistency of the joints. If joints are persistent (i.e., joint lengths are relatively long), more regularly shaped blocks are likely to be formed.

In this subactivity, sufficient DDA models will be run to capture the effects of uncertainties associated with the joint information used. The results for displacement predictions at specific positions for all DDA runs will be statistically treated and represented. A sufficient number of DDA model runs will be made until an acceptable statistic for the predicted displacement distributions is achieved. These displacement distributions will be compared to the measured displacement data.

3.3.3 Preparation of Report

Results of Subtask 2C activities will be discussed in the Task 2 team meeting to be held in Washington, DC, in February 2002. A progress report will be prepared subsequently and submitted to NRC in fiscal year 2002.

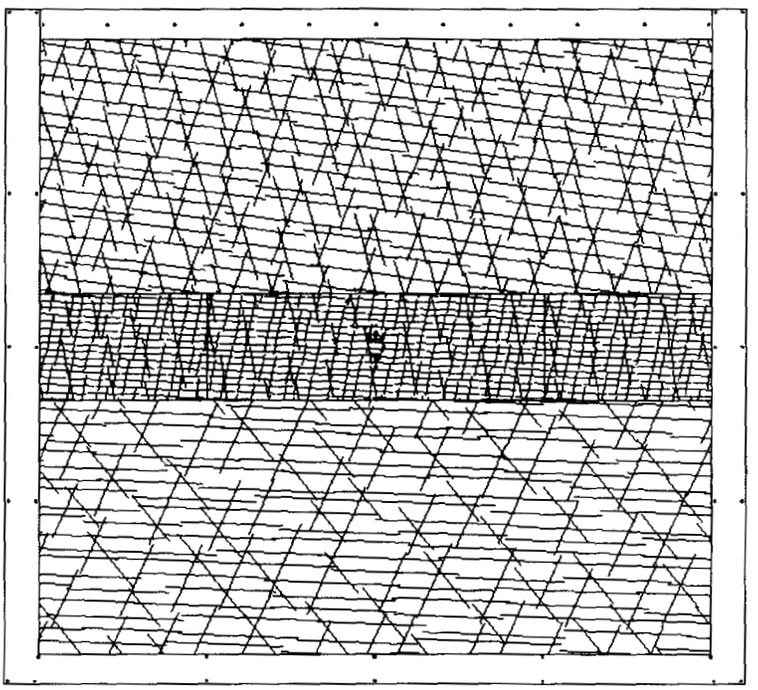

Figure 3-6. Joint Generation Realization 1

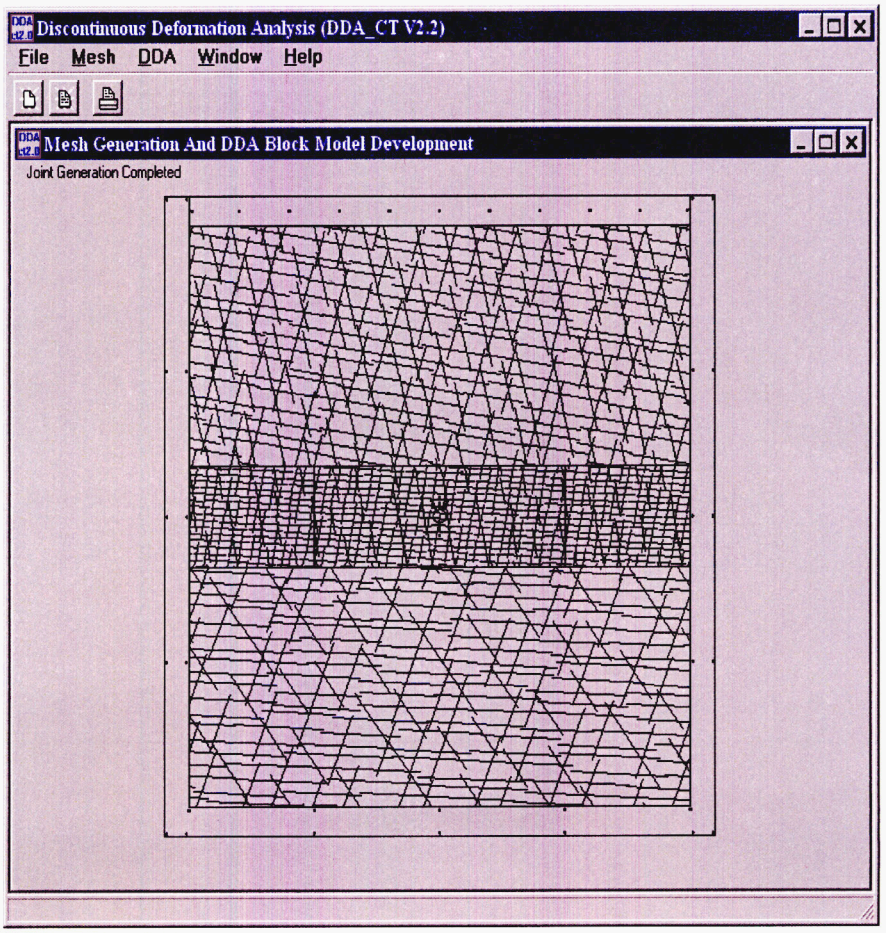

Figure 3-7. Joint Generation Realization 2

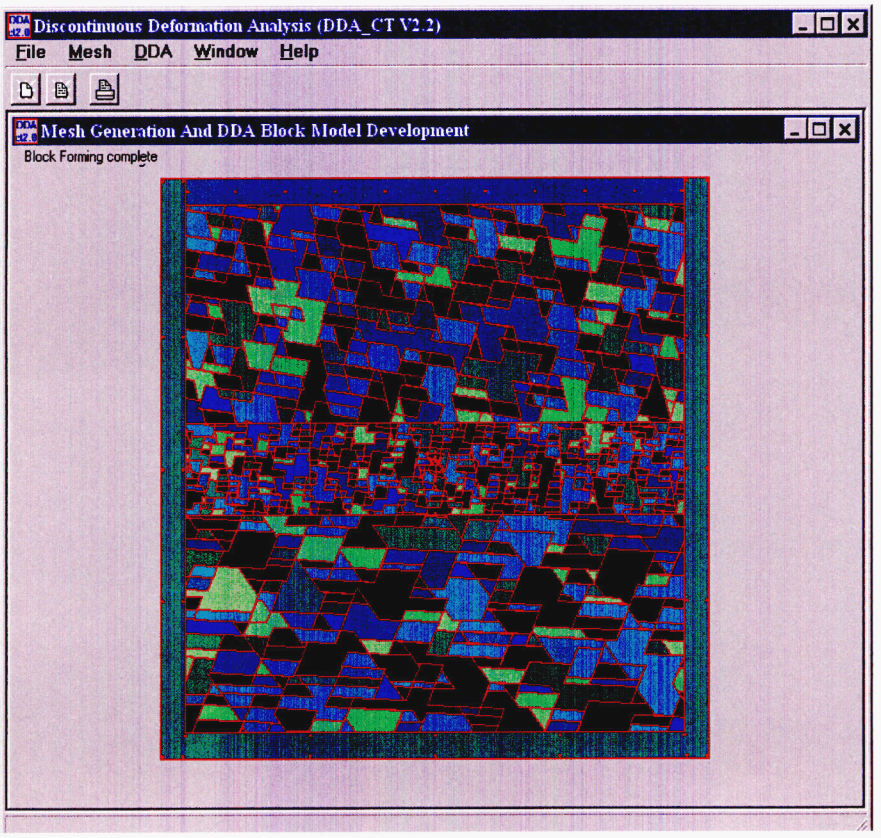

Figure 3-8. Discontinuous Deformation Analysis Block Model 2

4 SUMMARY

The drift-scale heater test at the Exploratory Studies Facility at Yucca Mountain is being analyzed in Task 2 of the DECOVALEX II project. Task 2 contains four subtasks. Subtask 2A is for thermal-hydrological modeling. Both Subtasks 2B and 2C are related to thermal-mechanical modeling, with 2B using the temperature generated from Subtask 2A, and 2C using the measured temperatures in the field. The last subtask examines thermal-hydrological-chemical modeling. The NRC/CNWRA research team is involved in Subtasks 2A and 2C modeling activities. Analysis for Subtask 2A has been completed. A report documenting the progress on Subtask 2A was submitted to NRC and to the DECOVALEX Secretariat in May 2001.

After completion of the thermal-hydrological analysis of the drift-scale heater test in Subtask 2A in May 2001, the preliminary activities for Subtask 2C began late in fiscal year 2001. This progress report is in the form of a work plan for the Subtask 2C activities. It is decided that both continuum and discontinuum approaches will be used for thermal-mechanical modeling of Subtask 2C. This technical approach has been presented at the DECOVALEX III Annual Workshop in Naantali, Finland, October 22–26, 2001. The ABAQUS finite element computer program will be used for continuum analysis and the dda_ct2 discontinuous deformation analysis computer code for discontinuum analysis.

The work for Subtask 2C includes four major activities: (i) development of numerical models, (ii) compilation of material and strength properties data, (iii) production of numerical analyses, and (iv) preparation of reports.

The numerical models to be developed for both continuum and discontinuum analyses will include three generalized lithologic zones: Topopah Spring upper lithophysal zone on the top, Topopah Spring middle nonlithophysal zone in the middle, and Topopah Spring lower lithophysal zone on the bottom. Some effort may be made in developing the finite element models to ensure that displacement prediction points are located on finite element nodes for ease of comparison with the measured data. Development of numerical models for DDA will rely on joint geometrical information from the geological mapping data collected from the Exploratory Studies Facility. The joint spacings and joint lengths will be scaled up to reduce the complexity of the problem.

The *in-situ* deformation moduli for the three lithologic zones will be determined based on rock-mass classification methods. The strength properties will be estimated based on the Hoek-Brown failure criterion for the continuum analysis and on the Coulomb failure criterion for the discontinuum analysis. Uncertainties associated with both material and strength properties will be quantified. The effects of these uncertainties on displacement prediction will be evaluated for the continuum analysis, and the uncertainties of the joint geometrical information will be assessed to determine their effects on rock-mass behavior in the discontinuum analysis.

Because data on joint stiffness and joint strength properties for the repository rock block are limited, a combination of the joint material properties from different sources will be used to develop necessary data input for discontinuous deformation analysis.

Both continuum and discontinuum analyses will be performed at three discrete heating times: 364, 730, and 1,002 d. Furthermore, failure of elements or blocks is allowed for both analyses. After failure, the finite elements in the continuum analysis exhibit perfectly plastic behavior, while the blocks break into four pieces under shear failure and into two pieces under tensile failure for the discontinuum analysis.

5 REFERENCES

Barton, N.R., R. Lien, and J. Lunde. "Engineering Classification of Rock Masses for the Design of Tunnel Support." *Rock Mechanics.* Vol. 6, No. 4. pp. 189–239. 1974.

Bieniawski, Z.T. "Rock Mass Classification in Rock Engineering." *Exploration for Rock Engineering.* Proceedings of the Symposium. Z.T. Bieniawski, ed. Vol. 1. pp. 97–106. Cape Town, South Africa: Balkema. 1976.

Bieniawski, Z.T. *Engineering Rock Mass Classifications.* New York City, New York: Wiley and Sons. 1989.

Chen, G. and Y. Ohnishi. "Practical Computing Formulas of Simplex Integration." Proceedings of the Third International Conference on Analysis of Discontinuous Deformation from Theory to Practice. B. Amadei, ed. Alexandria, Virginia: American Rock Mechanics Association. pp. 75–84. 1999.

CRWMS M&O. "Ambient Characterization of the Drift-Scale Test Block." BADD00000–01717–5705–00001. Revision 01. Las Vegas, Nevada: CRWMS M&O. 1997a.

———. "Drift Scale Test Design and Forecast Results." BAB000000–01717–4600–00007. Revision 1. Las Vegas, Nevada: CRWMS M&O. 1997b.

———. "Yucca Mountain Site Geotechnical Report." B00000000–01717–5705–00043. Vol. 1. Revision 01. Las Vegas, Nevada: CRWMS M&O. 1997c.

———. "Drift Degradation Analysis." ANL–EBS–MD–000027. Revision 01. Las Vegas, Nevada: CRWMS M&O. 2000a.

———. "Fracture Geometry Analysis for the Stratigraphic Units of the Repository Host Horizon." ANL–EBS–GE–000006. Revision 00. Las Vegas, Nevada: CRWMS M&O. 2000b.

Green, R.T., M.E. Hill, and S.L. Painter. "Progress Report for DECOVALEX III Task 2: Numerical Simulation of the Drift-Scale Heater Test at Yucca Mountain." San Antonio, Texas: CNWRA. 2001.

Hoek, E. and E.T. Brown. "Practical Estimated of Rock Mass Strength." *International Journal of Rock Mechanics and Mining Sciences.* Vol. 34, No. 8. pp. 1,165–1,186. 1997.

Hoek, E., P.K. Kaiser, and W.F. Brawden. *Support of Underground Excavations in Hard Rock.* Rotterdam, The Netherlands: Balkema. 1995.

Hsiung, S.M. "Discontinuous Deformation Analysis (DDA) with n^{th} Order Polynomial Displacement Functions." *Rock Mechanics in the National Interest.* Vol. 2. D. Elsworth, J.P. Tinucci, and K.A. Heasley, eds. Swets & Zeitlinger B.V.: Lisse, The Netherlands. pp. 1,413–1,420. 2001.

Hsiung, S.M., D.D. Kana, M.P. Ahola, A.H. Chowdhury, and A. Ghosh. NUREG/CR–6178. "Laboratory Characterization of Rock Joints." Washington, DC: NRC. 1994.

Itasca Consulting Group, Inc. "UDEC—Universal Distinct Element Code, Version 3.1." Minneapolis, Minnesota: Itasca Consulting Group, Inc. 2000.

Ma, M.Y. "Development of Discontinuous Deformation Analysis: The First Ten Years (1986 to 1996)." Proceedings of the Third International Conference on Analysis of Discontinuous Deformation (ICADD–3) from Theory to Practice. B. Amadei, ed. Alexandria, Virginia: American Rock Mechanics Association. pp. 17–32. 1999.

Ofoegbu, G.I. "Thermal-Mechanical Effects on Long-Term Hydrological Properties at the Proposed Yucca Mountain Nuclear Waste Repository." CNWRA 2000–03. San Antonio, Texas: CNWRA. 2000.

Shi, G.H. "Block System Modeling by Discontinuous Deformation Analysis. Topics in Engineering." *Computational Mechanics Publications*. C.A. Brebbia and J.J. Conner, eds. Vol. 11. Southampton, Great Britain: Computational Mechanics Publications. 1993.

———. "Modeling Dynamic Rock Failure by Discontinuous Deformation Analysis with Simplex Integration." Proceedings of the First North American Rock Mechanics Symposium, Austin, Texas. P.P. Nelson and Laubach, S.E., eds. Rotterdam, The Netherlands: Balkema. pp. 591–599. 1994.

———. "Discontinuous Deformation Analysis—Technical Note." First International Forum on Discontinuous Deformation Analysis, Berkeley, California. Vicksburg, Mississippi: Waterways Experiment Station, U.S. Army Corps of Engineers. 1996.

———. "Discontinuous Deformation Analysis User's Manual." Belmont, California: G.H. Shi. 1998.